Inorg. Chem. **2005**, *44*, 2524–2530

Cyclic Polyvanadates Incorporating Template Transition Metal Cationic Species: Synthesis and Structures of Hexavanadate $[PdV_6O_{18}]^{4-}$, Octavanadate $[Cu_2V_8O_{24}]^{4-}$, and Decavanadate $[Ni_4V_{10}O_{30}(OH)_2(H_2O)_6]^{4-}$

Taisei Kurata, Akira Uehara, Yoshihito Hayashi,* and Kiyoshi Isobe

Department of Chemistry, Kanazawa University, Kanazawa 920-1192, Japan

Received September 7, 2004

Three types of heteropolyvanadates, $[(C_2H_5)_4N]_4[PdV_6O_{18}]$ (**1**), $[(C_2H_5)_4N]_4[Cu_2V_8O_{24}]$ (**2**), and $[(C_6H_5)_4P]_4[Ni_4V_{10}O_{30}(OH)_2(H_2O)_6]$ (**3**), were synthesized through the reaction between the $[VO_3]^-$ anion and metal template cations of Pd(II), Cu(II), and Ni(II). The X-ray crystal structures of **1** ($a = 29.952(4)$ Å, $b = 12.911(2)$ Å, and $c = 13.678(2)$ Å, orthorhombic, space group $Pca2_1$ with $Z = 4$), **2** ($a = 13.740(1)$ Å, $b = 22.488(2)$ Å, $c = 18.505(2)$ Å, and $\beta = 94.058(2)°$, monoclinic, space group $P2_1/n$ with $Z = 4$), and **3** ($a = 12.333(2)$ Å, $b = 16.208(4)$ Å, $c = 16.516(3)$ Å, $\alpha = 112.438(3)°$, $\beta = 94.735(3)°$, and $\gamma = 104.749(3)°$, triclinic, space group $P\bar{1}$ with $Z = 1$) demonstrate that the metal cationic species induced cyclic $[VO_3]_n^{n-}$ ($n = 6$, 8, 10) ring formation and the cations are incorporated in the rings themselves. In the metal inclusion products, the cyclic vanadates act as macrocyclic ligands, in which the metal cationic species act as the templates. The cyclic vanadate is composed of tetrahedral VO_4 units that share corners and incorporates a metal cationic species in the center of the molecules. The bowl-shaped complex **1** includes a Pd^{2+} cation that is coordinated by the oxygen donors of a boatlike hexavanadate ring. The diamagnetic complex **1** was characterized via ^{51}V and ^{17}O NMR spectroscopy. Complex **2** involves an octavanadate ring and two Cu^{2+}, which are located on both sides of the mean plane as defined by the eight oxygen atoms that bridge the vanadium atoms. In the case of complex **3**, the di-μ-hydroxo-bridged Ni^{2+} dimer with capped Ni^{2+} aqua ions is formed by hydrolysis to form the decavanadate ring, in which two of the tetrahedral vanadate units are not bonded to the Ni^{2+} core but supported by hydrogen bonds through the aqua-ligand in the capped Ni^{2+} cation. Complexes **1**–**3** in solution were clearly identified by their characteristic isotope patterns using ESI-MS studies.

Introduction

Heteropolyoxometalates have received considerable attention due to their unique structures as well as their numerous applications toward chemical catalysis, materials science, and medicine.[1] Heteropolyanions are assembled by fusing MO_6 octahedrons around a heteroatom. Notable examples include the Keggin and Dawson anions with an $M'O_4$ tetrahedral heteroatom and the Anderson anion with an $M'O_6$ octahedral heteroatom.[2] Among the Anderson-type anions, and due to the open framework, the cyclic polyoxometalates with various heteroatoms bound within the ring are especially interesting as catalysis and separation tools.[3] Unfortunately, the rigid nature of the octahedral array of these Anderson anions limits the catalytic activity on the central atom and the reversible binding of the heteroatom. Recently, a new class of inorganic nanostructures with cyclic or spherical shape has been synthesized by Müller's group using self-assembly and templates.[4] To the best of our knowledge, however, heteropolyoxometalates anions assembled by fused MO_4 tetrahedrons incorporating heteroatoms are currently unknown.

Polyoxovanadates are expected to form flexible ring structures through tetrahedral arrays. Cyclic trivanadate $[V_3O_9]^{3-}$ and cyclic tetravanadate $[V_4O_{12}]^{4-}$ have been

* Author to whom correspondence should be addressed. E-mail: hayashi@cacheibm.s.kanazawa-u.ac.jp.

(1) Polyoxometalate Chemistry: From Topology via Self-Assembly to Applications; Pope, M. T., Müller, A., Eds.; Kluwer Academic Publishers: Dordrecht, Netherlands, 2001.
(2) Pope, M. T. *Heteropoly and Isopoly Oxometalates*; Springer-Verlag: Berlin, 1983.
(3) (a) Khan, M. I.; Tabussum, S.; Doedens, R. J. *Chem. Commun.* **2003**, 532−533. (b) Hasenknopf, B.; Delmont, R.; Herson, P.; Gouzerh, P. *Eur. J. Inorg. Chem.* **2002**, 1081−1087. (c) Golhen, S.; Ouahab, L.; Grandjean, D.; Molinie, P. *Inorg. Chem.* **1998**, *37*, 1499−1506.
(4) (a) Müller, A.; Peters, F.; Pope, M. T.; Gatteschi, D. *Chem. Rev.* **1998**, *98*, 239−271. (b) Müller, A.; Beckmann, E.; Bogge, H.; Schmidtmann, M.; Dress, A. *Angew. Chem., Int. Ed.* **2002**, *41*, 1162−1163.

10.1021/ic048751f CCC: $30.25
Published on Web 03/05/2005

isolated and confirmed by crystallographic studies.[5,6] Mechanistic details on the formation of these condensed species from $[VO_3]^-$, however, are difficult to elucidate because the $[VO_3]^-$ species in organic solvents are sensitive to slight changes in the experimental conditions, such as the type of cations, water content, and basicity of the solution, and can be transformed into unknown species. Although the presence of cyclic pentamer $[V_5O_{15}]^{5-}$ and hexamer $[V_6O_{18}]^{6-}$ in water has been indicated by solution studies,[7] cyclic vanadates larger than the V_4 unit have yet to be isolated and structurally characterized. Herein, we describe the synthesis and crystal structure of these larger cyclic host molecules that consist of VO_4 units. The molecules are formed in organic solvents by the cyclic oligomerization of $[VO_3]^-$ species. To facilitate the formation of the larger cyclic species, metal cationic species are employed as an effective template in the oligomerization of several $[VO_3]^-$ units around the species. The resulting complexes $[(C_2H_5)_4N]_4[PdV_6O_{18}]$ (**1**), $[(C_2H_5)_4N]_4[Cu_2V_8O_{24}]$ (**2**), and $[(C_6H_5)_4P]_4[Ni_4V_{10}O_{30}(OH)_2(H_2O)_6]$ (**3**) define a new class of cyclic vanadates that feature novel macrocyclic coordination chemistry between polyoxovanadates and various metal cationic species. These inorganic crown-ether-type inclusion complexes can potentially extract transition metal cations selectively within their ring cavities.

Experimental Section

Reagents, Solvents, and General Procedures. The following chemicals were purchased from commercial sources and were used without further purification: V_2O_5 (Wako); 40% $[(C_4H_9)_4N]OH$ aqueous solution (Aldrich); 20% $[(C_2H_5)_4N]OH$ aqueous solution (Wako); $Ni(NO_3)_2{\cdot}6H_2O$ (Katayama); $Cu(NO_3)_2{\cdot}3H_2O$ (Nacalai); $PdCl_2$ (Kojima); $[(C_6H_5)_4P]Br$ (Wako); $[(C_2H_5)_4N]Br$ (Wako); CH_3CN (Kanto); C_6H_5CN (Nacalai); $C_2H_5OC_2H_5$ (Nacalai). $[(n\text{-}C_4H_9)_4N]VO_3$,[8] $[(C_2H_5)_4N]VO_3$,[9] and $[Pd(C_6H_5CN)_2Cl_2]$[10] were prepared according to the literature methods.

Preparation of $[(C_2H_5)_4N]_4[PdV_6O_{18}]$ (1). A mixture of $[(C_2H_5)_4N]VO_3$ (140 mg, 0.6 mmol) and $[Pd(C_6H_5CN)_2Cl_2]$ (36 mg, 0.1 mmol) in acetonitrile (2 cm^3) was stirred for 1 min. The resulting orange solution was allowed to stand for 1 day at 25 °C to afford the product as orange crystals (70 mg, yield 58%, based on Pd). Anal. Calcd for $C_{34}H_{85}N_5O_{19}PdV_6$: C, 31.90; H, 6.69; N, 5.47. Found: C, 31.68; H, 6.65; N, 5.42. IR (Nujol, 500−1000 cm^{-1}): 954(s), 927(s), 854(sh), 831(s), 779(s), 721(w), 690(m). ^{51}V NMR (CH_3CN): δ −499 (4V), −565 (2V). ^{17}O NMR (CH_3CN): δ 517 (6 O), 618 (4 O), 1059 (8 O).

Preparation of $[(n\text{-}C_4H_9)_4N]_4[Cu_2V_8O_{24}]$ (2a). A solution of $[(n\text{-}C_4H_9)_4N]VO_3$ (136 mg, 0.4 mmol) in acetonitrile (0.5 cm^3) was added to the solution of $Cu(NO_3)_2{\cdot}3H_2O$ (24 mg, 0.1 mmol) in acetonitrile (0.5 cm^3). After the mixture was stirred for 1 min, to the resulting green solution was added 1 cm^3 of ether, and the mixture was allowed to stand for 1 day at 25 °C. Green crystals of $[(C_4H_9)_4N]_4[Cu_2V_8O_{24}]$ were obtained (86 mg, yield 91%, based on Cu). Anal. Calcd for $C_{64}H_{144}N_4Cu_2O_{24}V_8$: C, 40.70; H, 7.61; N, 3.00. Found: C, 40.76; H, 7.88; N, 2.86. IR (Nujol, 500−1000 cm^{-1}): 1001(sh), 962(s), 953(s), 897(vs), 873(m), 835(s), 721(w), 655(s), 580(w).

Preparation of $[(C_2H_5)_4N]_4[Cu_2V_8O_{24}]$ (2b). A solution of crystalline $[(n\text{-}C_4H_9)_4N]_4[Cu_2V_8O_{24}]$ in acetonitrile (1 cm^3) was added to a solution of $[(C_2H_5)_4N]Br$ (30 mg, 0.14 mmol) in acetonitrile (1 cm^3). After standing 1 day, green crystals of $[(C_2H_5)_4N]_4[Cu_2V_8O_{24}]$ were obtained from the mixture (18 mg, yield 25%, based on Cu). Anal. Calcd for $C_{32}H_{80}N_4Cu_2O_{24}V_8$: C, 26.70; H, 5.60; N, 3.89%. Found: C, 26.58; H, 5.77; N, 4.07. IR (Nujol, 500−1000 cm^{-1}): 1000(m), 968(s), 958(s), 943(m), 900-(vs), 869(m), 839(s), 786(w), 723(w), 667(s), 655(s), 584(w).

Preparation of $[(C_6H_5)_4P]_4[Ni_4V_{10}O_{30}(OH)_2(H_2O)_6]$ (3). A solution of $[(n\text{-}C_4H_9)_4N]VO_3$ (136 mg, 0.4 mmol) in acetonitrile (0.5 cm^3) was added to a solution of $Ni(NO_3)_2{\cdot}6H_2O$ (30 mg, 0.1 mmol) in acetonitrile (0.5 cm^3). After the mixture was stirred for 1 min, a small amount of solid in the mixture was removed by filtration. The filtrate was added to a solution of $[(C_6H_5)_4P]Br$ (50 mg, 0.12 mmol) in acetonitrile (0.5 cm^3), and then the mixture was allowed to stand for 24 h at 25 °C. Yellow crystals of $[(C_6H_5)_4P]_4[Ni_4V_{10}O_{30}(OH)_2(H_2O)_6]$ were obtained from the mixture (60 mg, yield 88%, based on Ni). Anal. Calcd for $C_{96}H_{110}Ni_4O_{46}P_4V_{10}$: C, 40.02; H, 3.87. Found: C, 39.97; H, 3.95. IR (Nujol, 1000−500 cm^{-1}): 997(w), 983(m), 966(m), 944(m), 923(m), 881(m), 848(s), 833(s), 754(s), 721(s), 688(s), 647(s), 613(w), 586(sh), 574(sh), 526(w).

X-ray Crystallography. Intensity data for the crystal of complex **1** (orange prism, 0.30 × 0.10 × 0.05 mm), complex **2b** (green prism, 0.15 × 0.12 × 0.10 mm), and complex **3** (yellow prism, 0.28 × 0.10 × 0.05 mm) were collected at −150 °C on a Rigaku/MSC Mercury diffractometer with graphite monochromated Mo Kα radiation (λ = 0.71070 Å) using 0.5° ω-scans at 0° and 90° in ϕ. Information on data collection and structure refinement, including the final cell constants, is listed in Table 1.

Based on a statistical analysis of intensity distribution, and on the successful solution and refinement of the structure, the space groups were determined as $Pca2_1$ for **1**, $P2_1/n$ for **2b**, and $P\bar{1}$ for **3**.

Data were collected and processed using the CrystalClear program (Rigaku). Semiempirical absorption corrections based on equivalent reflections were applied.[11] The data were corrected for Lorentz and polarization effects.

The structure was solved by direct methods (SHELXS-86).[12] The non-hydrogen atoms were refined anisotropically. Hydrogen atoms were included but not refined. The SHELXL-97 program was used for full-matrix least-squares refinement.[13] The final R_1 and wR_2 values were 0.072 and 0.125 for **1**, 0.052 and 0.107 for **2b**, and 0.043 and 0.104 for **3**, respectively.

The maximum and minimum peaks on the final difference Fourier map corresponded to 1.04 and −0.85 $e^-/Å^3$ for **1**, 0.77 and −0.81 $e^-/Å^3$ for **2b**, and 0.86 and −0.59 $e^-/Å^3$ for **3**, respectively.

All calculations were performed using the teXsan crystallographic software package (Molecular Structure Corp.).[14]

(5) Roman, P.; San Jose, A.; Luque, A.; Gutierrez-Zorrilla, J. M. *Inorg. Chem.* **1993**, *32*, 775−776.
(6) Hamilton, E. E.; Fanwick, P. E.; Wilker, J. J. *J. Am. Chem. Soc.* **2002**, *124*, 78−82.
(7) (a) Andersson, I.; Pettersson, L.; Hastings, J. J.; Howarth, O. W. *J. Chem. Soc., Dalton Trans.* **1996**, 3357−3361. (b) Tracey, A. S.; Jaswal, J. S.; Angus-Dunne, S. J. *Inorg. Chem.* **1995**, *34*, 5680−5685.
(8) Day, V. W.; Klemperer, W. G.; Yagasaki, A. *Chem. Lett.* **1990**, 1267−1270.
(9) Kawanami, N.; Ozeki, T.; Yagasaki, A. *J. Am. Chem. Soc.* **2000**, *122*, 1239−1240.
(10) Doyle, J. R.; Slade, P. E.; Jonassen, H. B. *Inorg. Synth.* **1960**, *6*, 218.
(11) *CrystalClear* ver. 1.3.5; Rigaku Corp.: Woodlands, TX, 1999.
(12) Sheldrick, G. M. *SHELXS-97*; University of Goettingen: Goettingen, Germany, 1997.
(13) Sheldrick, G. M. *SHELXL-97*; University of Goettingen: Goettingen, Germany, 1997.
(14) *teXsan: Crystal Structure Analysis Package*; Molecular Structure Corp.: The Woodland, TX, 1985 and 1999.

Table 1. Crystal Data for $[(C_2H_5)_4N]_4[PdV_6O_{18}]\cdot CH_3CN\cdot H_2O$ (**1**), $[(C_2H_5)_4N]_4[Cu_2V_8O_{24}]\cdot 2H_2O$ (**2**), and $[(C_6H_5)_4P]_4[Ni_4V_{10}O_{30}(OH)_2(H_2O)_6]\cdot 2CH_3CN\cdot 2H_2O$ (**3**)

compound	**1**	**2**	**3**
formula	$C_{34}H_{85}N_5O_{19}PdV_6$	$C_{32}Cu_2H_{84}N_4O_{26}V_8$	$C_{100}H_{104}N_2Ni_4O_{40}P_4V_{10}$
fw	1212.10	1471.62	2842.02
crystal system	orthorhombic	monoclinic	triclinic
space group	$Pca2_1$	$P2_1/n$	$P\bar{1}$
a, Å	29.952 (4)	13.740 (1)	12.333 (2)
b, Å	12.911 (2)	22.488 (2)	16.208 (4)
c, Å	13.678 (2)	18.505 (2)	16.516 (3)
α, deg	90	90	112.438 (3)
β, deg	90	94.058 (2)	94.735 (3)
γ, deg	90	90	104.749 (3)
V, Å	5289 (1)	5703.3 (8)	2890 (1)
Z	4	4	1
T, K	123(3)	123(3)	123(3)
μ (Mo Kα), cm^{-1}	14.13	20.54	15.4
reflections [$I > 2\sigma(I)$]	4878	4677	10 394
parameters	577	703	721
R_1 [$I > 2\sigma(I)$][a]	0.072	0.052	0.043
wR_2[b]	0.125	0.107	0.104
GOF	0.98	0.83	1.09

[a] $R_1 = \sum||F_o| - |F_c|/\sum|F_o||$. [b] $wR_2 = \{[\sum w(F_o^2 - F_c^2)^2]/\sum w(F_o^2)^2\}\}^{1/2}$.

Measurements. Infrared spectra were measured in mineral oil on a HORIBA FT-720 infrared spectrometer. All NMR samples were measured in CH_3CN solution at 25 °C. ^{51}V NMR spectra were recorded on a JEOL JNM-LA400 at 105.04 MHz. Chemical shifts were externally referenced to neat $VOCl_3$ ($\delta = 0$ ppm). A 10-μs pulse width and 10-μs preacquisition delay were used for all ^{51}V NMR measurements. ^{17}O NMR spectra were recorded on a JEOL JNM-LA400 at 54.23 MHz referenced to H_2O ($\delta = 0$ ppm). A 10-μs pulse width and 15-μs preacquisition delay were used for ^{17}O NMR measurements. Electrospray mass spectra in the negative mode were recorded on a micromass LCT mass spectrometer. An acetonitrile solution was directly injected at the flow rate of 600 μL/min. The tip of the capillary and the sampling cone were maintained at potentials of −1400 and −2 V, respectively. The source temperature was 25 °C. The m/z values refer to the highest peak of the ion clusters.

Results and Discussion

Synthesis. The reaction of $[VO_3]^-$ with metal cationic species in acetonitrile was found to be a viable synthetic route to afford cyclicvanadate complexes, $[VO_3]_n^{n-}$, which can serve as a macrocyclic oxygen donor toward metal cationic species at the center of the ring. Acetonitrile, rather than water, was employed as the solvent to avoid precipitation of the metal hydroxides and further hydrolysis of $[VO_3]^-$ species. The overall stoichiometry of the reactions is summarized in eq 1.

$$a[VO_3]^- + bM^{n+} \rightarrow [M_b^{n+}(VO_3)_a]^{n\times b-a} \quad (1)$$

Initially, the reaction of $[VO_3]^-$ with copper nitrate in acetonitrile was carried out to yield complex **2a**, which was crystallized directly from the reaction mixture by the addition of ether into the acetonitrile solution. Suitable crystals for X-ray structural analysis were obtained by the exchange of the countercation to afford the tetraethylammonium salt.

$$8[(n\text{-}C_4H_9)_4N][VO_3] + 2Cu(NO_3)_2 \rightarrow [(n\text{-}C_4H_9)_4N]_4[Cu_2V_8O_{24}] + 4[(n\text{-}C_4H_9)_4N]NO_3 \quad (2)$$

Our results show that the cyclic vanadate moiety is directly complexed to Cu^{2+}, with a molecular ratio of $[(C_2H_5)_4N][VO_3]$ to $Cu(NO_3)_2$ as 4:1. Using this reaction ratio, complex **2a** was prepared in 91% yields and in high purity.

To examine the metal selectivity of the ring and the relationship between metal and the ring size, our synthetic methodology was extended to other metal cyclic vanadate complexes. Cyclic polyoxovanadates were successfully formed using the Ni^{2+} and Pd^{2+} templates. In the case of Ni^{2+}, the formation of a light yellow solution yielded $[Ni_4V_{10}O_{30}(OH)_2(H_2O)_6]^{4-}$ as yellow crystals.

$$10[(n\text{-}C_4H_9)_4N][VO_3] + 4Ni(NO_3)_2 + 8H_2O \rightarrow [(n\text{-}C_4H_9)_4N]_4[Ni_4V_{10}O_{30}(OH)_2(H_2O)_6] + 6[(n\text{-}C_4H_9)N]NO_3 + 2HNO_3 \quad (3)$$

Occasionally, the crude solid included a small impurity, which was identified as Ni^{2+} hydrolysis products. Addition of an excess of the $[VO_3]^-$ salt resulted in the conversion of the hydrolysis species to the expected cyclic compound. Crystals suitable for X-ray structural analysis were obtained as the tetraphenylphosphonium salt by the exchange of the countercation in acetonitrile.

In Pd^{2+}, a mixture of $[(C_2H_5)_4N]VO_3$ and bis(benzonitrile)-dichloropalladium(II) afford cyclic hexavanadate with a molecular ratio of $[(C_2H_5)_4N]VO_3$ to $Pd(C_6H_5CN)_2Cl_2$ as 6:1.

$$6[(C_2H_5)_4N][VO_3] + Pd(C_6H_5CN)_2Cl_2 \rightarrow [(C_2H_5)_4N]_4[PdV_6O_{18}] + 2[(C_2H_5)_4N]Cl + 2C_6H_5CN \quad (4)$$

For this reaction, a precursor with labile benzonitrile ligands was essential. Use of organometallic Pd^{2+} compounds, such as dichloro(cyclooctadiene)palladium(II), resulted in a formation of a mixed valence decavanadate, $[V_{10}O_{26}]^{4-}$. The reaction of $[(C_4H_9)_4N]VO_3$ with di-μ-chlorobis(2-methylallyl)dipalladium(II) is known to afford mixed valence decavanadate through the tetravanadate-supported organometallic complex.[15]

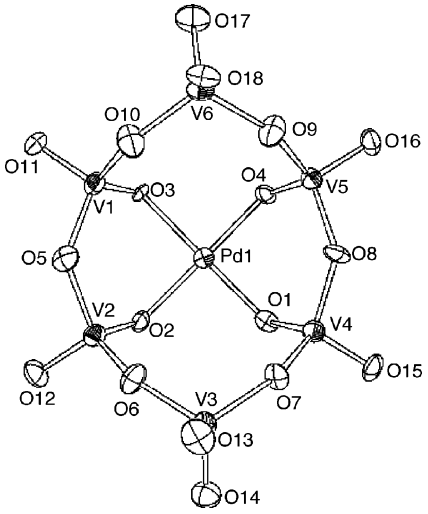

Figure 1. Structure of the $[PdV_6O_{18}]^{4-}$ anion in **1** with 50% probability thermal ellipsoids and the labeling scheme for all atoms.

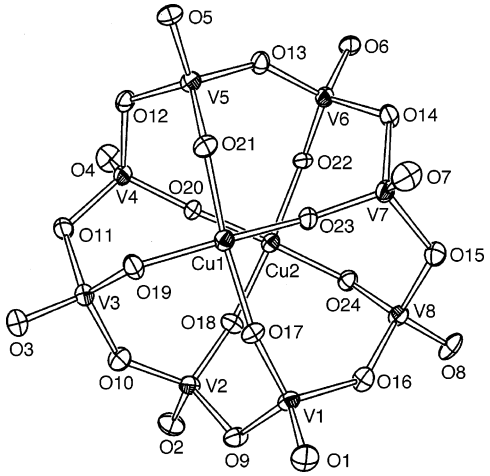

Figure 2. Structure of the $[Cu_2V_8O_{24}]^{4-}$ anion in **2b** with 50% probability thermal ellipsoids and the labeling scheme for all atoms.

Crystal Structure. The X-ray structural data for the three cyclic polyoxovanadates **1**, **2b**, and **3** are summarized in Figures 1−3 and Tables 2−4. The core of the anion of **1** can be described as a complex between Pd^{2+} and cyclic hexavanadate, $[VO_3]_6^{6-}$, composed of six tetrahedral VO_4 units bridged together through corner-sharing of the oxygen atoms. The hexavanadate ring exists in a boat conformation; two of the six VO_4 units at the flag positions are not coordinated to Pd^{2+}, thus leaving two terminal oxygen atoms per unit, whereas the remaining four VO_4 units are coordinated to Pd^{2+} through an oxygen atom, thus leaving one terminal oxygen per unit (Figure 1). The V−O distances that bridge between vanadium and Pd^{2+} ($V-O_{Pd}$, 1.687(8)−1.729(8) Å) are comparable to those that bridge between the vanadium atoms ($V-O_V$, 1.739(10)−1.835(9) Å) and longer than the terminal V−O distances ($V-O_{terminal}$, 1.597(8)−1.644(9) Å). The distances of the Pd−O bond range from 1.957(7) to 2.012(8) Å. The coordination sphere of Pd^{2+} is square plane (mean deviation = 0.04 Å).

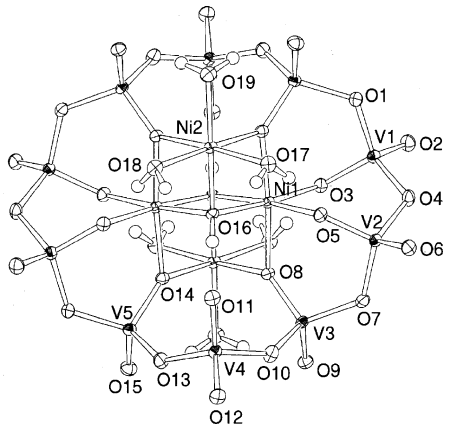

Figure 3. Structure of the $[Ni_4V_{10}O_{30}(OH)_2(H_2O)_2]^{4-}$ anion in **3** with 50% probability thermal ellipsoids and the labeling scheme for all atoms except hydrogen for clarity.

Table 2. Slected Bond Distances for $[(C_2H_5)_4N]_4[PdV_6O_{18}]$ (**1**)

Pd1−O1	1.975(7)	Pd1−O2	1.980(10)
Pd1−O3	2.006(7)	Pd1−O4	2.012(8)
V1−O1	1.724(8)	V1−O5	1.784(9)
V1−O10	1.771(10)	V1−O11	1.626(8)
V2−O2	1.729(9)	V2−O5	1.792(8)
V2−O6	1.764(8)	V2−O12	1.597(8)
V3−O6	1.820(8)	V3−O7	1.835(9)
V3−O13	1.644(9)	V3−O14	1.618(9)
V4−O3	1.723(8)	V4−O7	1.739(10)
V4−O8	1.834(9)	V4−O15	1.600(8)
V5−O4	1.687(8)	V5−O8	1.778(9)
V5−O9	1.757(9)	V5−O16	1.639(8)
V6−O9	1.824(9)	V6−O10	1.802(10)
V6−O17	1.629(10)	V6−O18	1.614(9)

Table 3. Selected Bond Distances for $[(C_2H_5)_4N]_4[Cu_2V_8O_{24}]$ (**2b**)

Cu1−O17	1.920(2)	Cu1−O19	1.910(2)
Cu1−O21	1.917(2)	Cu1−O23	1.901(2)
Cu2−O18	1.931(3)	Cu2−O20	1.896(2)
Cu2−O22	1.947(2)	Cu2−O24	1.912(2)
V1−O1	1.615(2)	V1−O9	1.795(2)
V1−O16	1.806(2)	V1−O17	1.673(2)
V2−O2	1.635(2)	V2−O9	1.806(2)
V2−O10	1.790(3)	V2−O18	1.673(3)
V3−O3	1.612(3)	V3−O10	1.788(2)
V3−O11	1.827(2)	V3−O19	1.681(2)
V4−O4	1.614(2)	V4−O11	1.799(3)
V4−O12	1.788(2)	V4−O20	1.693(2)
V5−O5	1.614(2)	V5−O12	1.808(2)
V5−O13	1.804(2)	V5−O21	1.695(2)
V6−O6	1.625(2)	V6−O13	1.790(2)
V6−O14	1.809(2)	V6−O22	1.680(2)
V7−O7	1.605(2)	V7−O14	1.796(2)
V7−O15	1.802(2)	V7−O23	1.686(3)
V8−O8	1.611(2)	V8−O15	1.822(2)
V8−O16	1.788(2)	V8−O24	1.688(2)

Similarly, the structure of complex **2b** (Figure 2) features a cyclic vanadate. In this case, cyclic octavanadate, $[VO_3]_8^{8-}$, incorporates two Cu^{2+} ions located on both sides of the mean plane defined by the eight V atoms. For each VO_4 tetrahedron, there is one corner-linked oxygen atom to Cu^{2+}, one free apex, and the two remaining oxygen atoms involved in the octavanadate ring.

Structurally, the Cu^{2+} inclusion complex and the mixed valence decavanadate, $[V_{10}O_{26}]^{4-}$, exist as similar shapes as defined by a crown ring of eight edge-shared tetrahedral VO_4 units.[16] The interior of both rings also contains similarly charged groups, that is, two Cu^{2+} in our compound or two

(15) Hayashi, Y.; Miyakoshi, N.; Shinguchi, T.; Uehara, A. *Chem. Lett.* **2001**, 170−171.

Table 4. Selected Bond Distances for $[(C_6H_5)_4P]_4[Ni_4V_{10}O_{30}(OH)_2(H_2O)_6]$ (**3**)

Ni1−O3	2.095(2)	Ni1−O5	2.075(2)
Ni1−O8	2.061(3)	Ni1−O14	2.068(3)
Ni1−O16	2.022(2)	Ni1−O16	2.011(2)
Ni2−O8	2.066(2)	Ni2−O14	2.047(2)
Ni2−O16	1.997(3)	Ni2−O17	2.089(2)
Ni2−O18	2.067(2)	Ni2−O19	2.083(3)
V1−O1	1.820(3)	V1−O2	1.613(2)
V1−O3	1.689(2)	V1−O4	1.814(3)
V2−O4	1.793(2)	V2−O5	1.687(2)
V2−O6	1.614(2)	V2−O7	1.833(3)
V3−O7	1.793(2)	V3−O8	1.691(2)
V3−O9	1.632(2)	V3−O10	1.781(2)
V4−O10	1.818(2)	V4−O11	1.642(3)
V4−O12	1.644(3)	V4−O13	1.808(2)
V5−O1	1.781(2)	V5−O13	1.789(3)
V5−O14	1.693(2)	V5−O15	1.629(3)

$[V^{IV}O]^{2+}$ in the mixed valence decavanadate; the total charge of −4 in both compounds is attained by the inclusion of two cations with charge of +2 within the $(VO_3)^{8-}$ ring. However, the symmetry of **2b** (C_s) is lower than that of the mixed valence decavanadate (S_8). The distortion of complex **2b** is best described by the angle between Cu^{2+} and the mean plane of the cyclic octavanadate. In the mixed valence decavanadate, the line through the two vanadium(IV) atoms is orthogonal to the least-squares plane of the eight oxygens bridging the vanadium. The angle between the line and the least-squares plane is about 80° in the **2b** polyanion. The V−O bond lengths in the bridge between the vanadium atoms (1.788(2)−1.827(2) Å) are longer than those that bridge vanadium and Cu^{2+} (1.673(2)−1.695(2) Å). The $V-O_{terminal}$ distances range from 1.605(2) to 1.635(2) Å, and the Cu−O bonds range from 1.896(2) to 1.947(2) Å.

The $[Ni_4V_{10}O_{30}(OH)_2(H_2O)_6]^{4-}$ anion is composed of a V_{10} ring and a central Ni^{2+} tetramer. The V_{10} ring is formed by 10 VO_4 units that share their tetrahedral corners. The central Ni^{2+} tetramer is formed by four NiO_6 units that share the edge of the octahedra. The V_{10} ring shares eight oxygen atoms with the central Ni^{2+} tetramer. The $[Ni_4V_{10}O_{30}(OH)_2(H_2O)_6]^{4-}$ anion has a symmetry of C_i.

The bond valence sums (BVS)[17] of oxygens in the $[Ni_4V_{10}O_{30}(OH)_2(H_2O)_6]^{4-}$ polyanion fall within 1.54−2.02, with the exception of O16, O17, O18, and O19. The bridging atom, O16, has a BVS value of 1.15 and therefore presumably corresponds to the hydroxo groups. The terminal oxygens (O17, O18, and O19) have significantly lower BVS values (0.31, 0.33, and 0.31, respectively), which correspond to the H_2O ligands. The bond distances of $V-\mu_2$-O (1.687(2)−1.833(3) Å) and $Ni-\mu_2$-O (2.075(2) and 2.095(2) Å) are longer than those of $V-\mu_3$-O (1.691(2) and 1.693(2) Å) and $Ni-\mu_3$-O (2.047(2)−2.068(3) Å), respectively. The $V-\mu_2$-O bond lengths in the bridge between the vanadium atoms (1.781(2)−1.833(3) Å) are longer than those in the bridge between vanadium and Ni^{2+} (1.687(2) and 1.689(2) Å). Distances of $V-O_{terminal}$ (1.613(2)−1.644(3) Å), Ni−OH (1.997(3)−2.022(2) Å), and $Ni-OH_2$ (2.067(2)−2.089(2) Å) are observed. While two of the ten VO_4 units from V_4 and the symmetry-related vanadium atom are not coordinated to Ni^{2+} tetramer leaving two terminal oxygen atoms per the unit, the remaining eight VO_4 units from V1, V2, V3, and V5 are coordinated to Ni^{2+} tetramer unit through an oxygen atom leaving one terminal oxygen atom per the units. The distances (2.82, 2.86, and 2.83 Å for O11···O16, O9···O19, and O15···O19, respectively) between the terminal oxygens of VO_4 tetrahedra and the oxygens of NiO_6 octahedra imply the presence of hydrogen bonds.

The size of the vanadate rings correlated with the total charge of the central metal ions. The higher the total charge of the central unit was, the larger the vanadate rings were formed. The presence of metal cationic species contributes to the decrease in a high charge density of larger cyclic vanadates $(VO_3)_n^{n-}$ that are sufficiently large to include metal cations within the ring. Thus, the addition of transition metal species to the $[VO_3]^-$ solution may drive the reaction toward the direction to form larger ring species. The metal cations act as a "template" in gathering the vanadate "ligands", and, similarly, the cyclic vanadate $(VO_3)_n^{n-}$ species can function as the macrocyclic oxo ligands. One of the oxo groups in each VO_3 unit that is directed inward can occupy the metal coordination sites on the template metal, thus leaving the second oxo group without coordination as a terminal oxygen. The bond valences of V−O distances were 1.54−1.75 ($V-O_{terminal}$), 1.22−1.42 (V−O(M)), and 0.92−1.19 (V−O(V)) for complexes **1**−**3**. The smaller bond valences of coordinated V−O(M) as compared to those of the terminal V−O shows that the interaction of cationic metal ion is not only electrostatic but also more specific, resulting in different sizes of the vanadate rings from the different metal ions with +2 charges.

^{51}V NMR. The interpretation of NMR spectra of the Pd^{2+} templated complex **1** is in agreement with that of the X-ray studies. The ^{51}V NMR spectrum of **1** in acetonitrile exhibits resonances at −499 and −565 ppm, with the intensity ratio of the downfield to the upfield peak of 2:1. The downfield peak was assigned to the vanadiums (V2, V3, V5, and V6) that were connected with Pd^{2+} through an oxygen bridge, whereas the upfield peak was assigned to the residual vanadiums (V1 and V4) at the flag position of the hexametallic boat-type conformation. These assignments were based on two factors: first, the existence of four vanadiums connected with Pd^{2+} and two vanadiums at the flag position is in accord with the intensity ratio, and, second, the ^{51}V NMR signal of a vanadium-supported noble metal complex tends to resonate downfield; the value of the chemical shift for the tetravanadate-supported organometallic compounds is in the range between −446 and −504 ppm.[8,15,18] In contrast, the chemical shift of the tetravanadate in acetonitrile is −570 and −574 ppm.[19] The hexametallic ring has two

(16) (a) Bino, A.; Cohen, S.; Heitner-Wirguin, C. *Inorg. Chem.* **1982**, *21*, 429−431. (b) Baxter, S. M.; Wolczanski, P. T. *Inorg. Chem.* **1989**, *28*, 3263−3264. (c) Heitner-Wirguin, C.; Selbin, J. *J. Inorg. Nucl. Chem.* **1968**, *30*, 3181−3188.

(17) Brown, I. D.; Altermatt, D. *Acta Crystallogr., Sect. B* **1985**, *B41*, 244−247.

(18) (a) Abe, M.; Isobe, K.; Kida, K.; Yagasaki, A. *Inorg. Chem.* **1996**, *35*, 5114−5115. (b) Abe, M.; Isobe, K.; Kida, K.; Nagasawa, A.; Yagasaki, A. *J. Cluster Sci.* **1994**, *5*, 565−571. (c) Abe, M.; Akashi, H.; Isobe, K.; Nakanishi, A.; Yagasaki, A. *J. Cluster Sci.* **1996**, *7*, 103−107.

possible conformations, boat and chair, which are attributable to the movements of V1 and V4. The conformation change of the hexametallic ring between the boat and chair conformations was not observed by variable-temperature ^{51}V NMR up to 75 °C. The ^{17}O NMR spectrum exhibited three resonances at 517, 618, and 1059 ppm, corresponding to the two types of bridging and terminal oxygens, respectively. The NMR spectra of complexes **2a** and **3** indicated paramagnetism of the corresponding Cu^{2+} and Ni^{2+} species and were not informative.

ESI Mass Spectrometry. The chemistry of vanadate in basic solution can be quite complex. The vanadate species that is formed from dissolving V_2O_5 in a strong basic solution is know as metavanadate with a chemical composition of $[VO_3]^-$. The study of the equilibriums of cyclic vanadate in the organic solution was reported by Peterson et al.;[7] furthermore, some of the representative cyclic species, tetravanadate $[V_4O_{12}]^{4-}$ and trivanadate $[V_3O_9]^{3-}$, have been isolated and confirmed by crystallographic studies.[6] $[V_4O_{12}]^{4-}$ is a predominant species in acetonitrile solutions, in which two types of structures have been reported, either the nonprotonated[5] or the protonated form.[20] Metavanadate-supported complexes have also been reported for organometallic groups of Rh, Ir, and Pd with a variety of organic ligands, such as η^4-C_6H_{10}, η^4-C_8H_{12}, η^4-C_8H_{14}, and η^3-allyl.[8,15,18] In these complexes, the two organometallic groups are bound to each side of the $[V_4O_{12}]^{4-}$ ring through the oxygens of two adjacent vanadiums. The supported organometallic complex demonstrates the ability of the vanadate oxo-group to coordinate and implies the potential of the vanadate groups as a macrocyclic oxo ligand. In these cyclic species, the framework is constructed by the cyclization of edge-shared tetrahedral VO_4 units.

To assess the VO_3^- species in acetonitrile under the conditions used for these experiments, ESI mass spectrometric studies were undertaken. Initially, the mass spectrum of the $(n\text{-}Bu_4N)VO_3$ was recorded as the reference spectrum. The chemical species of the metavanadate ion in an acetonitrile solution is known to exist as a mixture of cyclic trimers and tetramers. The mass spectrum of a 1 mM acetonitrile solution of $[(n\text{-}C_4H_9)_4N]VO_3$ supports the previous results[6] that cyclic trimers and tetramers coexist in the solution. However, cyclic hexamer, octamer, and decamer could not be detected (Figure 4 and Table 5). Mass spectra of complexes **1**, **2a**, and **3** show the formation of larger cyclic vanadates, in which the added metal cations play an important role as a template. The mass spectrum and the data of a 1 mM acetonitrile solution of complex **1** are shown in Figure 5 and Table 5, respectively. The peaks centered at $m/z = 236.4$ and 246.6 were assigned to the $\{[PdV_6O_{18}](CH_3CN)_n\}^{4-}$ ($n = 6$ and 7). The peaks centered at $m/z = 290.2$, 303.9, and 317.6 were assigned to the series of solvated $\{[(C_2H_5)_4N][PdV_6O_{18}](CH_3CN)_n\}^{3-}$ ($n = 1$, 2, and 3) species. $\{[(C_2H_5)_4N]H[PdV_6O_{18}]\}^{2-}$ and $\{[(C_2H_5)_4N]_2[PdV_6O_{18}]\}^{2-}$ were observed at $m/z = 415.3$ and 479.9, respectively. The mass spectrum of complex **2a** is similar to that of complex **1** (Figure 6 and Table 5). The peaks centered at $m/z = 270.4$, 280.6, and 290.9 were assigned to the solvated $[Cu_2V_8O_{24}]^{4-}$. The peaks centered

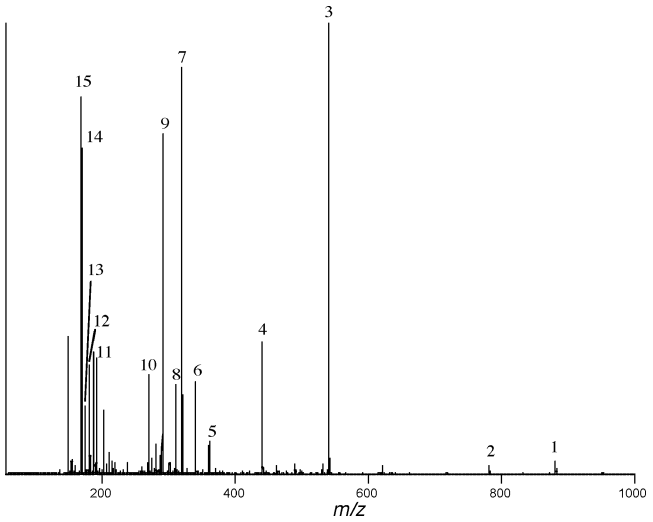

Figure 4. Mass spectrum of 1×10^{-3} M $[(n\text{-}C_4H_9)_4N]VO_3$ in acetonitrile.

Table 5. Assignment of Mass Spectral Data (Peak Numbers are According to Figures 4−7 in Each Complex)

peak number	ion	*m/z*
	$[(n\text{-}C_4H_9)_4N]VO_3$	
1	$\{[(n\text{-}C_4H_9)_4N]_2[HV_4O_{12}]\}^-$	881.4
2	$\{[(n\text{-}C_4H_9)_4N]_2[V_3O_9]\}^-$	781.4
3	$\{[(n\text{-}C_4H_9)_4N][HV_3O_9]\}^-$	540.1
4	$\{[(n\text{-}C_4H_9)_4N]_2[V_4O_{12}]\}^{2-}$	440.7
5	$\{[(n\text{-}C_4H_9)_4N][HV_4O_{12}](CH_3CN)_2\}^{2-}$	360.5
6	$\{[(n\text{-}C_4H_9)_4N][HV_4O_{12}](CH_3CN)\}^{2-}$	340.0
7	$\{[(n\text{-}C_4H_9)_4N][HV_4O_{12}]\}^{2-}$	319.5
8	$\{[(n\text{-}C_4H_9)_4N][V_3O_9](CH_3CN)_2\}^{2-}$	310.6
9	$\{[(n\text{-}C_4H_9)_4N][V_3O_9](CH_3CN)\}^{2-}$	290.1
10	$\{[(n\text{-}C_4H_9)_4N][V_3O_9]\}^{2-}$	269.6
11	$\{[HV_3O_9](CH_3CN)_2\}^{2-}$	189.9
12	$\{[V_3O_9](CH_3CN)_6\}^{3-}$	181.0
13	$\{[HV_4O_{12}](CH_3CN)_3\}^{3-}$	173.3
14	$\{[H_2V_2O_7](CH_3CN)_3\}^{2-}$	169.5
15	$\{[V_3O_9](CH_3CN)_5\}^{3-}$	167.3
	$[(C_2H_5)_4N]_4[PdV_6O_{18}]$	
1	$\{[(C_2H_5)_4N]_2[PdV_6O_{18}]\}^{2-}$	479.9
2	$\{[(C_2H_5)_4N]H[PdV_6O_{18}]\}^{2-}$	415.3
3	$\{[(C_2H_5)_4N][PdV_6O_{18}](CH_3CN)_3\}^{3-}$	317.6
4	$\{[(C_2H_5)_4N][PdV_6O_{18}](CH_3CN)_2\}^{3-}$	303.9
5	$\{[(C_2H_5)_4N][PdV_6O_{18}](CH_3CN)\}^{3-}$	290.2
6	$\{H[PdV_6O_{18}](CH_3CN)_2\}^{3-}$	260.8
7	$\{[PdV_6O_{18}](CH_3CN)_7\}^{4-}$	246.6
8	$\{[PdV_6O_{18}](CH_3CN)_6\}^{4-}$	236.4
	$[(n\text{-}C_4H_9)_4N]_4[Cu_2V_8O_{24}]$	
1	$\{[(n\text{-}C_4H_9)_4N]_2[Cu_2V_8O_{24}]\}^{2-}$	701.0
2	$\{[(n\text{-}C_4H_9)_4N]H[Cu_2V_8O_{24}]\}^{2-}$	580.3
3	$\{[(n\text{-}C_4H_9)_4N][Cu_2V_8O_{24}](CH_3CN)_2\}^{3-}$	413.9
4	$\{[(n\text{-}C_4H_9)_4N][Cu_2V_8O_{24}](CH_3CN)\}^{3-}$	400.2
5	$\{[(n\text{-}C_4H_9)_4N][Cu_2V_8O_{24}]\}^{3-}$	386.6
6	$\{[Cu_2V_8O_{24}](CH_3CN)_6\}^{4-}$	290.9
7	$\{[Cu_2V_8O_{24}](CH_3CN)_5\}^{4-}$	280.6
8	$\{[Cu_2V_8O_{24}](CH_3CN)_4\}^{4-}$	270.4
	$[(C_6H_5)_4P]_4[Ni_4V_{10}O_{30}(OH)_2(H_2O)_6]$	
1	$\{[(C_6H_5)_4P][Ni_4V_{10}O_{30}(OH)_2(H_2O)_2]\}^{3-}$	544.1
2	$\{H[Ni_4V_{10}O_{30}(OH)_2(H_2O)_5]\}^{3-}$	449.4
3	$\{H[Ni_4V_{10}O_{30}(OH)_2(H_2O)_4]\}^{3-}$	443.4
4	$\{[Ni_4V_{10}O_{30}(OH)_2(H_2O)_4](CH_3CN)_3\}^{4-}$	363.1
5	$\{[Ni_4V_{10}O_{30}(OH)_2(H_2O)_4](CH_3CN)_2\}^{4-}$	352.8
6	$\{[Ni_4V_{10}O_{30}(OH)_2(H_2O)_4](CH_3CN)\}^{4-}$	342.5

(19) Nakano, H.; Ozeki, T.; Yagasaki, A. *Acta Crystallogr., Sect. C* **2002**, *C58*, m464−m465.
(20) Fuchs, J.; Mahjour, S.; Pickardt, J. *Angew. Chem., Int. Ed. Engl.* **1976**, *15*, 374−375.

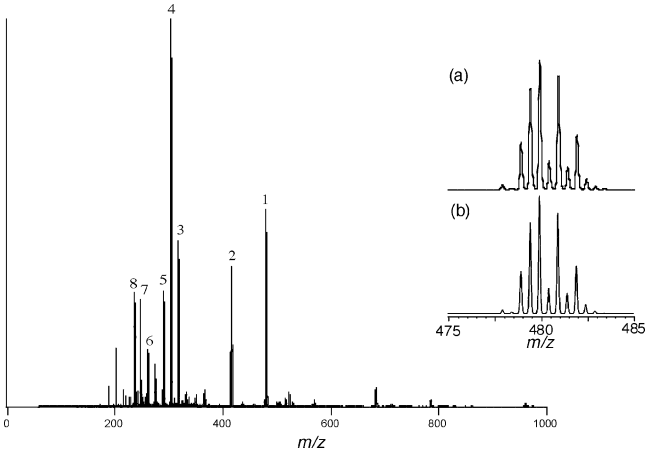

Figure 5. Mass spectrum of 1×10^{-3} M **1** in acetonitrile (see also Table 5 for the assignment of the envelopes with numbering). The insets show the isotopic distribution patterns of $\{[(C_2H_5)_4N]_2[PdV_6O_{18}]\}^{2-}$ with peak number 1 obtained experimentally (a) and from calculation (b).

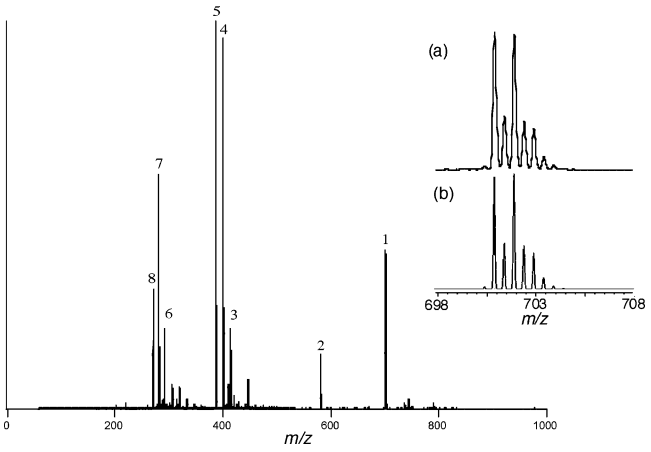

Figure 6. Mass spectrum of 1×10^{-3} M **2a** in acetonitrile (see also Table 5 for the assignment of the envelopes with numbering). The insets show the isotopic distribution patterns of $\{[(n\text{-}C_4H_9)_4N]_2[Cu_2V_8O_{24}]\}^{2-}$ with peak number 1 obtained experimentally (a) and from calculation (b).

at m/z = 386.6, 400.2, and 413.9 correspond to the solvated $\{[(n\text{-}C_4H_9)_4N][Cu_2V_8O_{24}]\}^{3-}$ species. $\{[(n\text{-}C_4H_9)_4N]H[Cu_2V_8O_{24}]\}^{2-}$ and $\{[(n\text{-}C_4H_9)_4N]_2[Cu_2V_8O_{24}]\}^{2-}$ were observed at m/z = 580.3 and 701.0, respectively. In contrast to those of complexes **1** and **2a**, the mass spectrum of complex **3** is more complicated because of the dissociation species of the aqua ligands in addition to the formation of the solvated species (Figure 7 and Table 5). The peaks centered at m/z = 342.5, 352.8, and 463.1 correspond to the solvated $[Ni_4V_{10}O_{30}(OH)_2(H_2O)_4]^{4-}$ species. The peaks centered at m/z = 443.4, 449.4, and 544.1 were assigned to $\{H[Ni_4V_{10}O_{30}(OH)_2(H_2O)_4]\}^{3-}$, $\{H[Ni_4V_{10}O_{30}(OH)_2(H_2O)_5]\}^{3-}$, and $\{[(C_6H_5)_4P][Ni_4V_{10}O_{30}(OH)_2(H_2O)_2]\}^{3-}$, respectively.

The ESI-MS spectra of the complexes **1** and **2** can be explained as the formation of two kinds of species: (1) the anionic species formed by the loss of cations from the cyclic parent compounds, and (2) the series of solvated anionic

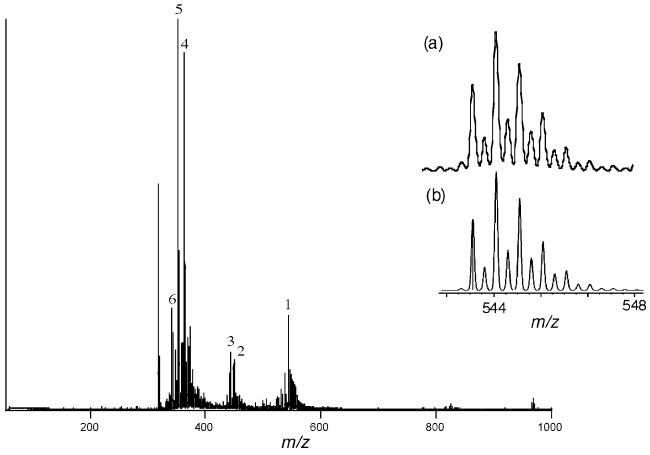

Figure 7. Mass spectrum of 3×10^{-4} M **3** in acetonitrile (see also Table 5 for the assignment of the envelopes with numbering). The insets show the isotopic distribution patterns of $\{[(C_6H_5)_4P][Ni_4V_{10}O_{30}(OH)_2(H_2O)_2]\}^{3-}$ with peak number 1 obtained experimentally (a) and from calculation (b).

complexes formed by acetonitrile. The ESI-MS spectra of complex **3** can also be explained by these species and the dissociated aqua species by the loss of the coordinated water molecule. Few fragmented species were observed. Applying higher potentials to the tip of the capillary and the sampling cone resulted in a more complex mass spectrum, indicating analytes such as cleaved species by the removal of template metals.

Our results indicate that the addition of the Lewis acid transition metal species shifts the condensation process toward the formation of a larger ring.

Conclusion

Structural studies of cyclic heteropolyoxovanadates incorporating metal cationic species have allowed us to gain insight into the metal template effect on the formation of the cyclic polyoxovanadate species in acetonitrile. Novel cyclic polyoxovanadates with three vanadate ring sizes were prepared by the reaction between the alkylammonium metavanadate and transition metal ions in acetonitrile. Cyclic hexavanadate was obtained from the reaction of tetraethylammonium metavanadate with bis(benzonitrile)dichloropalladium(II), whereas cyclic octavanadate and decavanadate were prepared by the treatment of tetrabutylammonium metavanadate with copper(II) nitrate and nickel(II) nitrate, respectively.

Our simple synthetic methodology for this new class of large inorganic macrocyclic coordination complexes can be extended for the synthesis of other polyoxovanadate ring complexes with different cationic groups and perhaps different ring sizes. Furthermore, it may prove to be interesting to explore reactions with larger cationic hydroxide species.

Supporting Information Available: Full details of crystallographic studies of **1**, **2**, and **3** in CIF format. This material is available free of charge via the Internet at http://pubs.acs.org.

IC048751F